Eur. Phys. J. B **29**, 485–489 (2002)
DOI: 10.1140/epjb/e2002-00329-0

THE EUROPEAN PHYSICAL JOURNAL B

Cellular oscillator with a small number of particles

V.P. Zhdanov[a]

Department of Applied Physics, Chalmers University of Technology, 412 96 Göteborg, Sweden
and
Boreskov Institute of Catalysis, Russian Academy of Sciences, Novosibirsk 630090, Russia

Received 21 April 2002 / Received in final form 19 June 2002
Published online 14 October 2002 –

Abstract. To illustrate complex spatio-temporal effects which are possible in cellular reactions with a small number of particles, we present Monte Carlo simulations of the formation of oscillatory spark-like patterns in a model completely stochastic Ca^{+2} oscillator. Our analysis shows that in order to observe such patterns the minimum average number of Ca^{+2} ions in the cytosol may be as low as about 50.

PACS. 05.10.Ln Monte Carlo methods – 05.40.-a Fluctuation phenomena, random processes, noise, and Brownian motion – 05.65.+b Self-organized systems – 87.17.-d Cellular structure and processes

1 Introduction

Chemical reactions in cells are usually described by employing the conventional mean-field (MF) kinetic equations based on the mass-action law [1]. This approach is often robust especially in the cases when a kinetic process under consideration exhibits well-defined steady-state behaviour. Frequently, however, the kinetics of biological processes occuring on subcellular, cellular or multi-cellular levels are oscillatory. More specifically, the experiments indicate that physiological rhythms are rarely strictly periodic but rather fluctuate irregularly over time [2]. To analyse such rhythms, one usually needs to take into account fluctuations in one form or another. The conventional approach tackling this aspect of reaction kinetics is based on complementing the MF reaction-diffusion equations by stochastic white noise. The latter approach is however not always applicable to cells, because the number of particles (molecules, atoms, or ions) participating in cellular processes is often small. The cell behaviour may be dependent on a few or even on a single particle which may switch intracellular biochemical pathways [3]. The firm understanding of kinetic effects corresponding to this limit is now lacking. The first simulations [4–6] addressing this point treat *temporal* stochastic reaction schemes with no concentration gradients. Monte Carlo (MC) simulations of irregular intracellular oscillations with concentration gradients have recently been performed in references [7,8], but the number of reacting particles was there relatively large. Our present study is focused on kinetically complex *spatio-temporal* cellular processes occurring with a small number of reactants and regulators.

Regulation of cell activity often involves positive and negative feedbacks between reactants and/or regulators and accordingly may result in periodic or irregular kinetic oscillations. The time scale of oscillations may be comparable with that characterizing reactant diffusion in a cell. Under such conditions, kinetic oscillations may be accompanied by pattern formation inside individual cells [9] (for example, glycolytic NAD(P)H waves have recently been observed in neutrophils [10]; another good example is Ca^{+2} waves monitored in *Xenopus* oocytes [11]). One of the questions naturally arising in connection with cellular spatio-temporal patterns is: *How low may be the minimum average number of reactants in the cell or cellular compartments in order to observe this phenomenon?* Referring to the fluctuation theory or, specifically, to the Poissonian distribution [12], one can argue that the very term "oscillations" becomes poorly defined if the number of reactants is lower than 30, because in this limit oscillations can hardly be distinguished from fluctuations. What kind of spatio-temporal patterns we may really have if the number of reactants is about or slightly larger than 30 remains however unclear. To address this question, we present MC simulations of oscillatory cellular patterns formed by a small number of particles.

2 Model

As an example, we construct and treat a completely stochastic model of the cellular Ca^{+2} oscillator. The understanding of Ca^{+2} oscillations is of interest from the practical point of view, because Ca^{+2} plays an important role in regulation of cell metabolism. From the theoretical viewpoint, this case is attractive, because despite

[a] e-mail: zhdanov@catalysis.nsk.su

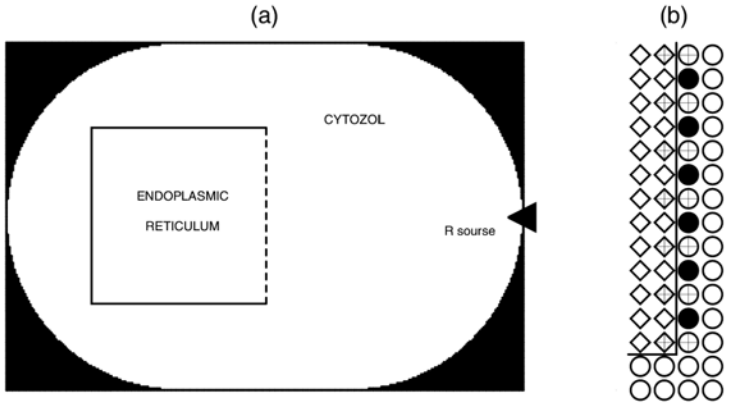

Fig. 1. (a) Elongated cell (white colour) on the lattice. The sites near the corners (black colour) do not belong to the cell. Ca^{+2} is supplied from the cytosol to ER primarily *via* the bottom, top and left ER-cytosol boundaries (solid lines). The right boundary (dashed line) contains channels for the Ca^{+2} exchange between the cytosol and ER. The filled triangle indicates location of the receptor responsible for R production. (b) Fragment of the ER-cytosol boundary with channels. The circles and diamonds show the sites belonging to the cytosol and ER, respectively. The sites mimicking the channels are marked by the plus signs (Ca^{+2} ions are allowed to cross the boundary *via* these sites). The filled circles represent the regulatory sites binding reversibly Ca^{+2} or R particles.

the complexity and diversity of cellular biochemical pathways in different cells there seem to exist a few general principles behind the control of Ca^{+2} concentration (see the review [9] and recent experiments [13] and/or simulations [14] based on the MF approximation or combining the MF approach with stochastic elements). (i) Oscillations occur primarily during exchange of Ca^{+2} between the cytosol and endoplasmic reticulum (ER) (the Ca^{+2} concentration in the cytosol is much lower than that in ER). (ii) Calcium release from ER is mediated by the membrane channels organized spatially in clusters. This process is autocatalytic (positive feedback), *i.e.*, its rate increases with increasing Ca^{+2} concentration in the cytosol. (iii) The channel-mediated Ca^{+2} transport is regulated by 1,4,5-trisphosphate or another regulator, R, which may be deactivated by Ca^{+2} or by other species formed due to the Ca^{+2} release (negative feedback). (iv) The Ca^{+2} supply from the cytosol to ER occurs primarily with participation of the Ca^{+2} ATP-pumps.

Realization of principles (i–iv) depends on the system under consideration. Taking into account the complexity and diversity of cellular biochemical systems, we have no ambition to describe in detail any specific system. Our goal is rather to construct a generic stochastic model focused on oscillations with a small number of Ca^{+2} ions. In our 2D MC simulations, the elongated cell is represented by an array of sites on a (300×200) square lattice (Fig. 1a). Each site can be either vacant or occupied by Ca^{+2} or R. ER is mimicked by a (101×101) sublattice located on the left side of the cell. 51 channels mediating the Ca^{+2} transport are formed by the sites on the right boundary of the sublattice as shown in detail in Figure 1b. The other 50 sites on the right boundary are able to bind reversibly Ca^{+2} or R particles. The bound species regulate the Ca^{+2} transport through the channels. The ATP-pumps are assumed to be located at random on the bottom, top and left ER-cytosol boundaries. In this case, there is no need to describe them explicitly. Instead, we prescribe to the bottom, top and left ER-cytosol boundary sites an effective probability of Ca^{+2} penetration from the cytosol to ER (this process is considered to be locally irreversible). Diffusion of Ca^{+2} and R particles occurs *via* jumps to nearest-neighbour (nn) vacant site. Deactivation of R particles is described as the $R + Ca^{+2} \rightarrow P + Ca^{+2}$ reaction between nn Ca^{+2} and R particles (in reality, R may be deactivated by other species formed due to the Ca^{+2} release, but this detail is not crucial for our conclusions). P particles are removed from the lattice immediately after reaction events. In addition, we introduce a receptor responsible for R production. The receptor is represented by one of the sites on the external boundary.

3 Algorithm of simulations

In MC simulations, the probabilities of elementary steps should be dimensionless. Practically, this means that the rate constants of various steps have to be normalized to the rate constant of the fastest step so that the probability of this step is equal to unity [15]. In our simulations, the fastest processes are considered to be Ca^{+2} and R diffusion. The probabilities of Ca^{+2} and R jumps to nn vacant sites are therefore set equal to unity (in reality, the rates of diffusion of these species are of course different, and this detail could be incorporated into the simulations, but it does not change the conclusions). The probabilities of the other steps are chosen as described below.

The algorithm of our simulations consists of trials to realize one of the elementary processes in the cell. A site

(site 1) belonging to the cell is chosen at random. Then, depending on its location and local arrangement of particles, there are three options:

(1) If site 1 is vacant and does not represent the receptor, the trial ends. The vacant receptor site is occupied by R with the probability $p_{\rm rec} < 1$ (this step mimics R production).

(2) If site 1 is occupied by Ca^{+2}, one of the nn site (site 2) is selected at random. If site 2 is occupied or does not belong to the cell, the trial ends. If site 2 is vacant, the events depend on location of sites 1 and 2 as follows. (i) If both sites are in ER or if both sites are in the cytosol and do not belong to the right ER-cytosol boundary, Ca^{+2} jumps from site 1 to site 2 with unit probability. (ii) If sites 1 and 2 form the bottom, top and left ER-cytosol boundary (this means that one of them belongs to the cytosol and another one to ER), Ca^{+2} jumps from site 1 to site 2 with the probability $p_{\rm pum} < 1$ provided that site 1 is in the cytosol (this step mimics the performance of the Ca^{2+} ATP-pumps). If site 1 belongs to ER, the trial ends. (iii) If sites 1 and 2 form the right ER-cytosol boundary, Ca^{+2} jumps from one site to another with the probability $p_{\rm ch} < 1$ provided that the sites form a channel. The jump is realized if the two nn (with respect to the channel) regulatory sites are occupied by Ca^{+2} or if at least one of these sites is occupied by R. If sites 1 and 2 do not form a channel, the trial ends. (iv) If sites 1 and 2 belong to the cytosol and one of them is regulatory, Ca^{+2} jumps from site 1 to site 2 with the probability $p_{\rm a}^{\rm Ca} < 1$ provided that site 2 is regulatory or with the probability $p_{\rm b}^{\rm Ca} < 1$ provided that site 1 is regulatory (to take into account that the regulatory sites bind Ca^{+2}, we use $p_{\rm b}^{\rm Ca} \ll p_{\rm a}^{\rm Ca}$).

(3) If site 1 is occupied by R, one of the nn site (site 2) is chosen at random. If site 2 is occupied by R, or belongs to CR, or is outside the cell, the trial ends. If site 2 is occupied by Ca^{+2}, R is removed from site 1 with the probability $p_{\rm dea}$ (this step mimics R deactivation). If site 2 is vacant, the events depend on whether one of the sites is regulatory or not. (i) If both sites are ordinary, R jumps from site 1 to site 2 with unit probability. (ii) If one of the sites is regulatory, R jumps from site 1 to site 2 with the probability $p_{\rm a}^{\rm R} < 1$ provided that site 2 is regulatory or with the probability $p_{\rm b}^{\rm R} < 1$ provided that site 1 is regulatory (in analogy with the rules for Ca^{+2}, we employ $p_{\rm b}^{\rm R} \ll p_{\rm a}^{\rm R}$).

Initially (at $t = 0$), Ca^{+2} ions are distributed in the cell at random with the average site occupancy $p_{\rm av} \ll 1$. In addition, we add a few (3–20) R particles on the sublattice representing the cytosol. Then, after each trial, the MC time is incremented by $\Delta t_{\rm MC} = |\ln(\xi)|/N_{\rm s}$, where $\xi \leq 1$ is a random number, and $N_{\rm s}$ the number of sites on the lattice representing the cell. On the average, we have $\langle|\ln(\xi)|\rangle = 1$. Thus, $\Delta t_{\rm MC} = 1$ corresponds to one trial per site or, in other words, to one MS step (MCS). Taking into account that the probabilities of Ca^{+2} and R jumps to nn vacant sites are considered to be equal to unity, we may also conclude that one MCS corresponds in reality to $\Delta t = a^2/4D$, where a is the lattice spacing and D the Ca^{+2} or R diffusion coefficient.

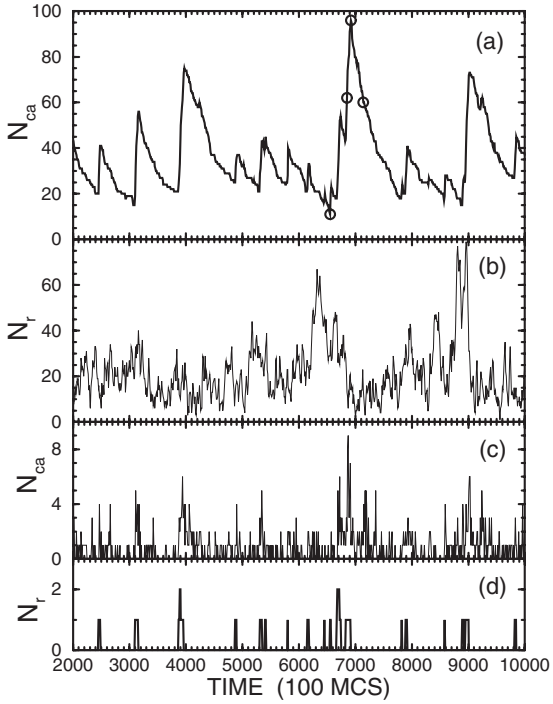

Fig. 2. Total numbers of (a) Ca^{+2} ions and (b) R particles in the cytosol and numbers of (c) Ca^{+2} ions and (d) R particles in regulatory sites on the ER-cytosol boundary as a function of time for $p_{\rm rec} = 0.01$, $p_{\rm pum} = 0.1$, $p_{\rm ch} = 0.2$, $p_{\rm a}^{\rm Ca} = 1$, $p_{\rm b}^{\rm Ca} = 0.1$, $p_{\rm a}^{\rm R} = 0.1$, $p_{\rm b}^{\rm R} = 0.001$, $p_{\rm dea} = 1$, and $p_{\rm av} = 0.02$. The data presented demonstrate the established asymptotic regime of kinetic oscillations. The transient stage (at $t < 2 \times 10^5$ MCS) is not shown. The interval between the data points is 10^3 MCS. The lattice snapshots corresponding to the points indicated by open circles [panel (a)] are exhibited below in Figure 3.

4 Results of simulations

During the simulations, we monitored the total numbers of Ca^{+2} and R particles in the cytosol and also the numbers of these particles in regulatory sites. Varying the kinetic parameters in a wide range, we have found that the model described easily exhibits well-developed irregular spark-like spatio-temporal oscillations of Ca^{+2} ions in the cytosol if the average value of the number of these ions is larger or about 40. The average number of R particles may be as low as about 20. An example of such oscillations is shown in Figure 2. In this case, the average number and amplitude of oscillations of the number of Ca^{+2} ions in the cytosol are about 35 and 20, respectively. For comparison, it is appropriate to note that according to the Poissonian distribution the amplitude of fluctuations of this number is expected to be lower than 10.

Comparing panels (a) and (b) of Figure 2, one can notice that due to the negative feedback between Ca^{+2} and R the concentrations of these species oscillate in the anti-phase regime. The rapid spark-like increase of Ca^{+2} concentration starts when the number of R particles is relatively high at the moment when one of these particles reaches a regulatory site (*cf.* panels (a) and (c) of Fig. 2). Then, with increasing Ca^{+2} concentration, the

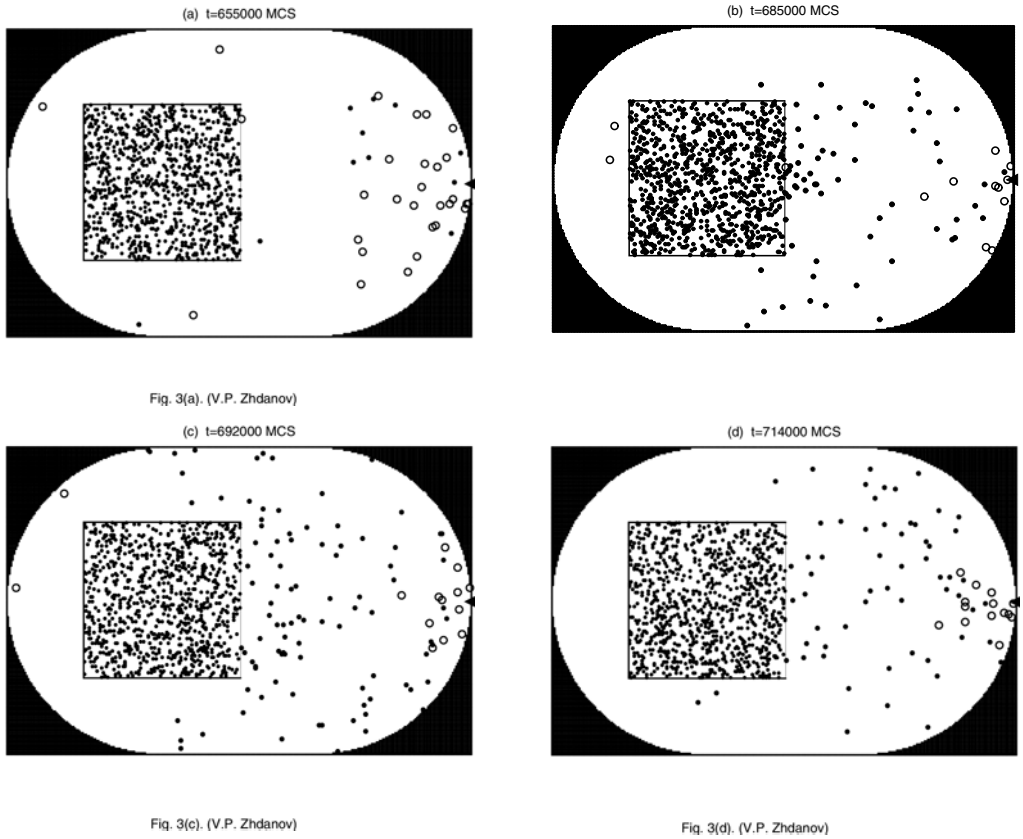

Fig. 3. Typical snapshots of the lattice for the MC run, shown in Figure 2, in the cases when the number of Ca^{+2} ions in the cytosol is (a) minimum, (b) between minimum and maximum, (c) maximum, and (d) between maximum and minimum. Small and somewhat larger filled circles represent Ca^{+2} ions in the ER and cytosol, respectively. Open circles indicate R particles. To increase resolution, the size of circles is used to be larger than the site size. For this reason, the concentration of Ca^{+2} ions in ER appears to be higher than it might be in the case when the sizes matched each other.

number of R particles rapidly decreases due to deactivation by Ca^{+2}. The growth of Ca^{+2} concentration is however maintained for a while due to autocatalysis (*cf.* panels a and c of Fig. 2). This process is however eventually terminated due to relatively slow diffusion of Ca^{+2} ions to regions located far from the channels and pumping them back to CR *via* the bottom, top and left ER-cytosol boundaries. All these events are illustrated in Figure 3.

The effect of some of the model parameters on irregular oscillations of the number of Ca^{2+} ions in the cytosol is demonstrated in Figures 4, 5. In particular, Figure 4 shows what we may have with further decrease of the average number of Ca^{+2} ions. For example, increasing the effective probability of Ca^{+2} penetration from the cytosol to ER *via* the bottom, top and left ER-cytosol boundary sites (from 0.1 to 0.5) results in reduction of the average number of Ca^{+2} ions down to about 25 (Fig. 4b). Despite the small number of Ca^{+2} ions, the spark-like features of the kinetics are still well manifested, because they are connected first of all with the interplay of the processes near the array of channels on the right side of ER. If one the other hand one decreases the probability of jumps *via* open channels (from 0.2 to 0.1), the average number of Ca^{+2} ions decreases down to about 25 as well (Fig. 4c), but now the amplitude of the oscillations is smaller (nearly the same as expected on the basis of the Poissonian distribution) and the shape of peaks is almost symmetric. Such kinetic behavior can be classified rather as fluctuations.

Figure 5 exhibits the kinetics with a higher average number of Ca^{+2} ions. In particular, Figure 5b corresponds to the case when the probability of R deactivation is decreased from 1 to 0.1. This results in increasing number of R particles. The average number of Ca^{+2} ions increases as well, but the amplitude of Ca^{+2} oscillations remains nearly the same (Figs. 5 a, b).

Figure 5c shows that spark-like oscillations are possible even if R production and degradation is eliminated and hence there is no negative feedback between R and Ca^{+2}.

Finally, it makes sense to compare quantitatively some predictions of our model with experiment. In our simulations, we employ dimensionless probabilities. To avoid a lengthy discussion of the relationship between these probabilities and real rate constants, we may use dimensionless values characterizing sparks. Specifically, it is of interest to calculate the dimensionless parameter $D\tau/\rho^2$, where D is the Ca^{+2} diffusion coefficient, and τ and ρ are the spark time and length scales. In our work, $D = 0.25$, $\tau \simeq 5\times10^4$, $\rho \simeq 100$, and accordingly $D\tau/\rho^2 \simeq 1$. In recent experi-

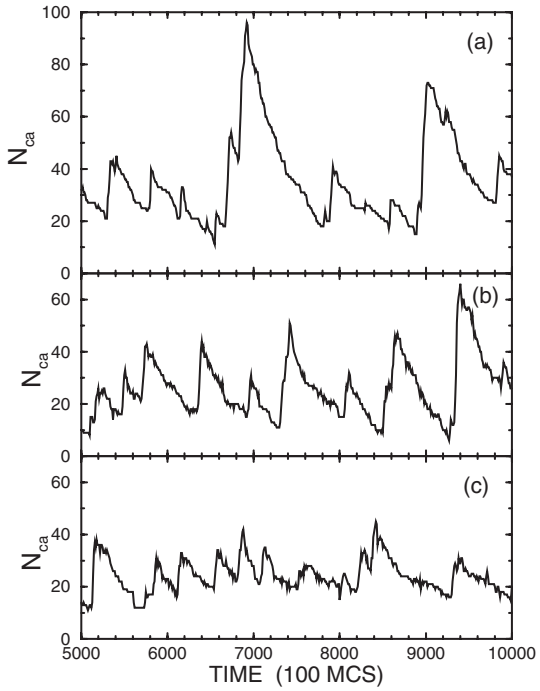

Fig. 4. Total numbers of Ca^{+2} ions in the cytosol as a function of time for (a) the run, shown in Figure 2, and [(b) and (c)] the runs with the same parameters as in Figure 2 except (b) $p_{\rm pum} = 0.5$ and (c) $p_{\rm ch} = 0.1$.

ment [13], $\tau \simeq 10^{-2}$ s and $\rho \simeq 5 \times 10^{-4}$ cm. Combining the latter values with $D \simeq 2 \times 10^{-6}$ cm^2/c [16], one gets $D\tau/\rho^2 \simeq 10^{-1}$. The experimental value is seen to be somewhat smaller, but the difference is acceptable especially if one takes into account that we did not use any fitting parameters and had no goal to describe in detail specific experiments.

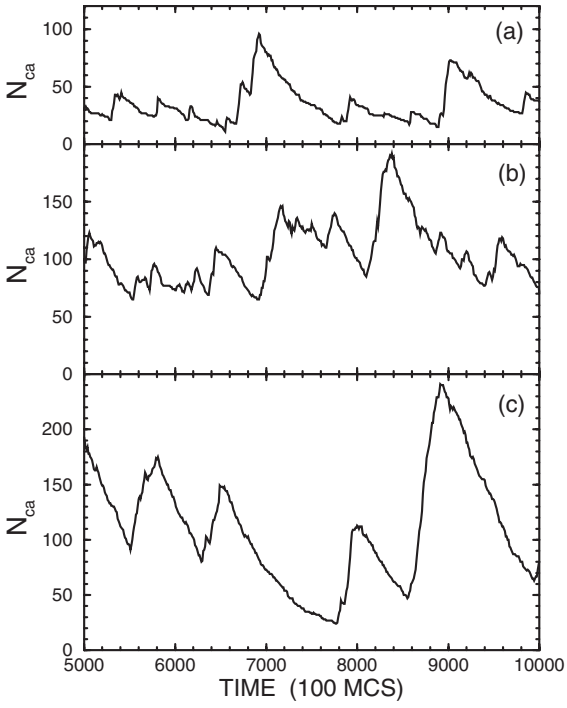

Fig. 5. Total numbers of Ca^{+2} ions in the cytosol as a function of time for (a) the run shown in Figure 2, (b) the run with the same parameters as in Figure 2 except $p_{\rm dea} = 0.1$, and (c) the run with three R particles and the same parameters as in Figure 2 except $p_{\rm rec} = 0$ and $p_{\rm dea} = 0$ (in this case, there is no R generation and deactivation).

5 Conclusion

We have constructed the first completely stochastic model of intracellular spark-like Ca^{+2} oscillations. The model allows one to explicitly simulate the effect of various factors on oscillations. Our present curiosity-driven simulations were focused on the case when the number of particles participating in oscillations is small. The results obtained demonstrate that oscillatory cellular spatio-temporal patterns may in principle be observed when the average number of reactants in the cell or cellular compartments is as low as about 50. We believe that this general conclusion may be useful for understanding and interpretation of various irregular physiological rhythms and/or such processes as neuronal dynamics.

The author thanks B. Kasemo for useful discussions.

References

1. H. Gutfreund, *Kinetics for the Life Sciences* (Cambridge University Press, Cambridge, 1995)
2. L. Glass, Nature **410**, 277 (2001)
3. H.H. McAdams, A. Arkin, Trends. Genet. **15**, 65 (1999)
4. J. Paulsson, O.G. Berg, M. Ehrenberg, Proc. Nat. Acad. Sci. USA **97**, 7148 (2000)

5. O.G. Berg, J. Paulsson, M. Ehrenberg, Biophys. J. **79**, 1228 (2000)
6. Y. Togashi, K. Kaneko, Phys. Rev. Lett. **86**, 2459 (2001)
7. V.P. Zhdanov, B. Kasemo, Phys. Chem. Chem. Phys. **3**, 3786 (2001)
8. V.P. Zhdanov, Intern. J. Bifurc. Chaos **12** (2002), in press
9. G. Dupont, S. Swellens, C. Clair, T. Tordjmann, L. Combettes, Biochim. Biophys. Acta - Molec. Cell Res. **1498**, 134 (2000)
10. H.R. Petty, R.G. Worth, A.L. Kindzelskii, Phys. Rev. Lett. **84**, 2754 (2000)
11. J. Marchant, I. Parker, EMBO J. **20**, 65 (2001) and references therein
12. L.D. Landau, E.M. Lifshitz, *Statistical Physics* (Pergamon, Oxford, 1993)
13. A. Gonzalez, W.G. Kirsch, N. Shirokova, G. Pizarro, G. Brum, I.N. Pessah, M.D. Stern, H. Cheng, E. Rios, Proc. Nat. Acad. Sci. USA **97**, 4380 (2000)
14. J. Keizer, G.D. Smith, Biophys. Chem. **72**, 87 (1998); M. Falcke, L.S. Tsimring, H. Levine, Phys. Rev. E **62**, 2636 (2000); T. Haberichter, M. Marhl, R. Heinrich, Biophys. Chem. **90**, 17 (2001)
15. K. Binder, in *Monte Carlo Methods in Statistical Physics*, edited by K. Binder (Springer, Berlin, 1979), p. 1
16. N.L. Allbritton, T. Meyer, L. Stryer, Science **258**, 1812 (1992)